Photocatalytic Oxidation of Methyl Mercaptan in Foul Gas for Odor Control

X. Z. Li,*,† M. F. Hou,†,‡ F. B. Li,‡ and H. Chua†

Department of Civil and Structural Engineering, The Hong Kong Polytechnic University, Hong Kong, China, and Guangdong Key Laboratory of Agricultural Environment Pollution Integrated Control, Guangdong Institute of Eco-Environment and Soil Science, Guangzhou 510650, China

Methyl mercaptan (CH_3SH) is a representative odorous pollutant from various odor emission sources such as sewage and municipal solid wastes. This study confirms that CH_3SH in a synthetic foul gas can be effectively decomposed by UV-C (<280 nm) photolysis using germicidal lamps, but is resistant to destruction under UV-A (365 nm) irradiation using black-light lamps. This study also demonstrates that CH_3SH in foul gas can be successfully degraded by photocatalytic oxidation under UV-A irradiation using TiO_2-based photocatalysts. In this study, two new catalysts, NH_4^+-modified TiO_2 (NH_4^+-TiO_2) and SO_4^{2-}-modified TiO_2 (SO_4^{2-}-TiO_2), were prepared by a precipitate-refluxing method and a hydrothermal method, respectively. These two catalysts as well as the commercially available catalyst Degussa P25 (P25-TiO_2) were used for the photocatalytic degradation of CH_3SH. It was found that the NH_4^+-TiO_2 catalyst achieved a better performance than P25-TiO_2, whereas SO_4^{2-}-TiO_2 demonstrated a poorer performance. The high photocatalytic activity of NH_4^+-TiO_2 for CH_3SH degradation results from its basic characteristics and the presence of an ammonium (NH_4^+) group on the NH_4^+-TiO_2 catalyst surface. The photocatalytic degradation of CH_3SH was further studied using the P25-TiO_2 catalyst under different experimental conditions. The experimental results showed that catalyst loading, relative humidity, and initial concentration could influence the efficiency of CH_3SH photocatalytic degradation significantly. It was found that a catalyst loading of 3.93 mg cm^{-2} and a relative humidity of 43% are two essential factors for achieving the best performance under these experimental conditions. This work provides new insights into the removal of a sulfur-containing organic substance (CH_3SH) from the gas phase by both photolysis and photocatalytic oxidation processes.

Introduction

Mercaptans (thiols) are odorous pollutants that are disagreeable to our environment.[1] Among thiols, methyl mercaptan (CH_3SH) is a representative odorous compound with significant toxicity and a very low odor threshold of around 0.4 ppb that arises mainly from natural sources, petroleum-refining processes, the wood-pulping industry, sewage treatment works, and energy-related activities.[2,3]

Removal of CH_3SH has been investigated by catalytic oxidation over cobalt(II) catalysts[4,5] or wood and coal fly ash,[6] adsorption and oxidation on activated carbons,[1] catalytic incineration over Pt/Al_2O_3 catalyst,[7] radiolytic decomposition in an RF plasma reactor,[3] and also some biological alternatives.[8] However, there are a variety of advantages and disadvantages of these techniques, and they showed different degrees of cost effectiveness.[9]

Recently, the degradation of odorous compounds by advanced oxidation processes (AOPs) have been found to be very effective.[10,11] Among AOPs, the photocatalytic oxidation of various organic compounds with TiO_2/UV has been proposed to be an attractive process for wastewater treatment and also air purification.[12−14] Various research works on the removal of pollutants from a foul gas initiated by semiconductor photocatalysis have been reported,[15,16] but few studies have investigated the photolysis and photocatalytic oxidation of CH_3SH by TiO_2/UV in the gas phase. It is necessary to carry out a systematic investigation of the photocatalytic oxidation of CH_3SH affected by different factors such as TiO_2 catalyst loading, relative humidity, and initial concentration of CH_3SH, which usually have critical influences on the gas−solid adsorption behavior and photocatalytic reaction.[17,18]

In the present work, the photolysis and photocatalytic oxidation of CH_3SH in the gas phase were investigated using different UV sources and three TiO_2-based catalysts to determine the effects of main factors on the performance of CH_3SH degradation in a laboratory-scale photoreactor system.

Experimental Section

Materials. CH_3SH gas with a traceable concentration of 2000 ppm in air was supplied by BOC Gases and used as an odorous gas source. A commercially available TiO_2 photocatalyst (P25-TiO_2) was purchased from Degussa AG Company, containing 30% rutile and 70% anatase with a primary particle size of 30 nm and a specific area of 50 ± 15 m^2 g^{-1}. These P25-TiO_2 particles are spherical and nonporous and have a purity of >99.5%. An NH_4^+-modified TiO_2 photocatalyst (NH_4^+-TiO_2) was prepared in our laboratory by a precipitate-refluxing method according to the following procedure: Tetra-*n*-butyl titanate (17 mL) was dissolved in 115 mL of absolute ethanol, and this solution was then added dropwise under vigorous stirring into a premixed solution (20 mL of 2 mol L^{-1} NH_3 in H_2O) at 343 K. The resulting suspension was stirred for 0.5 h. The precipitate was centrifuged from the above suspension, collected, and washed four times with distilled water. Then, the collected precipitate was added to 200 mL of 0.05 mol L^{-1} HNO_3 solution; the suspension was refluxed for 2 h at 343 K and then centrifuged to collect the precipitate. The precipitate was further washed four times with distilled water and dried in an oven for 24 h at 333 K to obtain the resulting NH_4^+-TiO_2 powder catalyst. A SO_4^{2-}-modified TiO_2 photocatalyst (SO_4^{2-}-TiO_2) was also prepared by a hydrothermal method according to the following

* To whom correspondence should be addressed. Tel.: +852-27666016. Fax: +852-23346389. E-mail: cexzli@polyu.edu.hk.

† The Hong Kong Polytechnic University.

‡ Guangdong Institute of Eco-Environment and Soil Science.

10.1021/ie050343b CCC: $33.50 © 2006 American Chemical Society
Published on Web 12/15/2005

procedure: Titanium sulfate was first mixed with distilled water to prepare a mixture with a concentration of 0.6 mol L^{-1}; then, the mixture was stirred for 10 min and aged in a PTFE-lined autoclave at 393 K for 12 h. After the autoclave had been quenched in cold water, the precipitate was collected, washed with distilled water five times, and then filtered and dried for 24 h at 378 K to obtain the resulting SO_4^{2-}-TiO_2 powder catalyst. The physicochemical properties of the two new catalysts were characterized by X-ray diffraction (XRD) for their crystalline structure and crystallinity, the BET method for their surface areas, and FTIR spectroscopy for information on their surface groups.

To prepare the photocatalyst-coated sheets for photocatalytic oxidation of CH_3SH in the gas phase, the above catalysts were first mixed with distilled water to make an aqueous suspension with a concentration of 3 wt %. Then, a Whatman glass fiber sheet with an area of 21 cm × 20 cm was used as a supporting medium, and the above catalysts were coated on the glass fiber by a dip-coating method, in which the supported catalyst was dried from room temperature to 378 K with a temperature gradient of 3.5 K/min for 3 h. The loading of catalyst was determined by a weight difference before and after the coating process. The catalyst loading of 3.93 mg cm^{-2} was used in most experiments, except the tests of the effect of catalyst loading.

Photoreactor Setup and Experimental Procedure. All experiments of photolysis and photocatalytic oxidation were conducted in a batch photoreactor with an effective volume of 33.4 L [29 cm (h) × 48 cm (l) × 24 cm (w)] that was made of Pyrex glass and had its inner surface coated with a Teflon film to eliminate any adsorption. Inside the photoreactor, three UV lamps were positioned at the upper level as a light source, and a TiO_2-coated glass fiber sheet with a size of 21 cm × 20 cm was horizontally placed on the Teflon film at the lower level. The distance between the UV lamps and TiO_2 catalyst was 5 cm. During the photolysis experiments, two types of UV lamps, three germicidal lamps (model G8T5, 8 W, Sankyo Denki Co. Ltd.) and three black-light lamps (model F8T5/BLB, 8 W, Xinyuan Co. Ltd.), were used. The wavelength of the germicidal lamp (low-pressure mercury lamp) was in the range of 200−280 nm with a maximum irradiation intensity at 254 nm as a UV-C irradiation source, and that of the black-light lamp was in the range of 310−400 nm with a maximum irradiation intensity at 365 nm as a UV-A irradiation source. A methyl mercaptan sensor (Cole-Parmer, model DM-100-CH_3SH) is equipped inside the photoreactor to monitor the CH_3SH concentration during experiments. This methyl mercaptan analyzer has a measurement range of 0−100 ppm (detection limit = 0.1 ppm, repeatability = 2% of signal). To obtain reliable experimental data, each experiment was repeated three times under same experimental conditions, and the average value of the CH_3SH readings from the methyl mercaptan sensor was adopted to determine the CH_3SH concentration with a deviation of 0.5%. A complete setup of this photoreactor system is shown in Figure 1.

Whereas the CH_3SH gas was used as a foul gas source, a zero air generator (Thermo Environmental Inc., model 111) was used to supply a clean air stream as an odor-free gas source. After passing through a humidity-control chamber, the odor-free air gas was well mixed with the CH_3SH gas in a gas mixing chamber to formulate a synthetic foul gas with different initial CH_3SH concentrations and was then purged into the photoreactor before the experiments. The initial relative humidity (RH) of the reaction gas was controlled in the range of 30−80%. During the photolysis of CH_3SH, the UV lamps were turned on after the desired concentration of CH_3SH had been introduced into the photoreactor. In photocatalytic experiments, after the synthetic foul gas had been purged into the photoreactor, the concentration of CH_3SH was gradually reduced through adsorption by the catalyst. It took a few hours to reach a gas−solid adsorption/desorption equilibrium, before the lamps were turned on for the photocatalytic oxidation reaction. In the experiments, once the CH_3SH reading from the sensor changed at a rate of <0.5 ppm/h, it was believed that a state of CH_3SH adsorption/desorption equilibrium on the surface of catalyst had been reached.

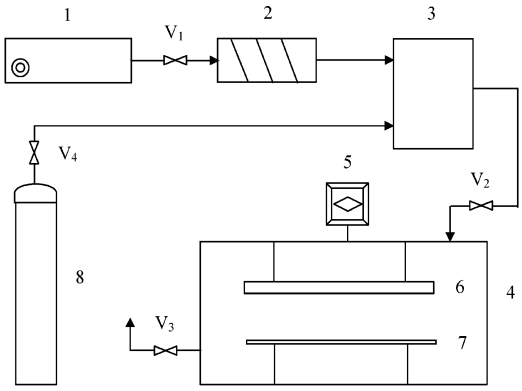

1-Zero air generator, 2-Humidification chamber, 3-Reactant gases mixing chamber, 4-Photo batch reactor, 5-CH_3SH sensor, 6-lamps, 7-supported catalyst, 8-CH_3SH gas cylinder, V_1, V_2, V_3 and V_4 –Valves

Figure 1. Schematic representation of the experimental apparatus.

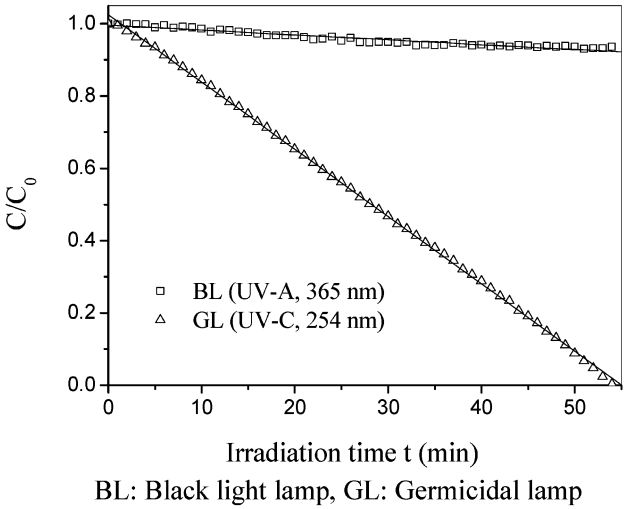

Figure 2. Photolysis of CH_3SH with different irradiation sources.

Results and Discussion

Photolysis of CH_3SH under Different UV Illuminations. In this study, two sets of photolysis experiments were carried out first by using different UV irradiation sources, in which CH_3SH gas at an initial concentration of 94 ppm was irradiated by either three germicidal lamps or three black-light lamps to conduct photolysis reactions with a relative humidity of 60% at room temperature. Each photolysis reaction lasted for 55 min, and the results are shown in Figure 2 and Table 1. The experimental results demonstrated that CH_3SH was effectively reduced by photolysis under UV-C irradiation (I = 2.58 mW cm^{-2} at 254 nm) provided by three germicidal lamps. Almost 100% removal of CH_3SH was achieved after 55 min of reaction.

Table 1. Kinetic Data for the Photolysis of CH_3SH (C_0 = 94 ppm)

	light intensity (mW cm^{-2})		zeroth-order kinetics	
light source[a]	254 nm	365 nm	k_0 (g m^{-3} s^{-1})	R
three GLs	2.58	0.077	0.0186	0.9998
three BLs	0	1.280	0.0013	0.9639

[a] GLs = germicidal lamps, BLs = black-light lamps.

However, the experimental results also showed that the reduction of CH_3SH was insignificant under UV-A irradiation (I = 1.28 mW cm^{-2} at 365 nm) provided by three black-light lamps.

The photochemistry of CH_3SH has been reported by several studies.[19,20] CH_3SH has a light absorption spectrum mainly below 280 nm.[21] During the photolysis of CH_3SH in the range of 185−254 nm, the dominant photochemical process leads to breakage of the S−H bond,[21,22] but not the C−S bond, even though the C−S bond is considerably weaker than the S−H bond (72.4 ± 1.5 vs 86.1 ± 0.6 kcal mol^{-1}, respectively).[23]

$$CH_3SH + h\nu \rightarrow CH_3S\bullet + H\bullet \quad (1)$$

It has also been reported that the photolysis occurs on the excited potential energy surface, repulsive in the S−H coordinate, rather than on the ground-state surface, where the weakest bond-breaking channels would be expected to dominate. To date, the UV photolysis of CH_3SH has been studied under low-wavelength irradiation with most of the focus on the reaction mechanism, not the purification of foul air in the environment. Moreover, there is a lack of studies about the effects of different irradiation sources. Because the photolysis of CH_3SH under the UV irradiation at 200−280 nm is very fast and creates the radicals $CH_3S\bullet$ and H• (eq 1), then the radicals can react with oxygen or water to produce SO_2, H_2 and H_2S. The reaction mechanism can be summarized as follows:[24,25]

$$CH_3SH + H\bullet \rightarrow H_2 + CH_3S\bullet \text{ or } CH_3SH + H\bullet \rightarrow H_2S + CH_3\bullet \quad (2)$$

$$H\bullet + O_2 \rightarrow HO_2\bullet \quad (3)$$

$$HO_2\bullet + nCH_3SH \rightarrow nCH_3S\bullet + SO_2 \quad (4)$$

It has been reported that, in the absence of O_2, the photolysis of CH_3SH at 253.7 nm and 296 K gives H_2, $(CH_3S)_2$, CH_4, and H_2S (eq 2) as products.[24] However, when O_2 is present, the products from the photolysis of CH_3SH include SO_2, H_2, and H_2S (eqs 2−4).[24] The experimental results in this study have confirmed that the UV-C photolysis process could realize fast and almost complete degradation of CH_3SH using the germicidal lamps. However, there was little degradation of CH_3SH by photolysis under the UV-A irradiation derived from the black-light lamps. The absorption spectrum of CH_3SH shows two prominent bands centered around 230 and 205 nm, and the photoexcitation and subsequent dissociation of methyl mercaptan (CH_3SH) occur significantly with irradiation around its absorption bands.[19] Because the emission of black-light lamps lies in the range of 310−400 nm, there was insignificant photolysis of CH_3SH using this UV irradiation source.

Characteristics of Photocatalysts. The two new catalysts NH_4^+-TiO_2 and SO_4^{2-}-TiO_2 were first examined by XRD to determine their crystalline structure and crystallinity and then by the BET method to determine their surface areas and further by FTIR spectroscopy to identify some surface groups. The XRD patterns showed that both the NH_4^+-TiO_2 and SO_4^{2-}-TiO_2 catalysts were predominantly anatase TiO_2, but their crystallinities were much lower than that of P25-TiO_2, as shown in Table 2. The BET results indicated that the surface areas of NH_4^+-TiO_2 and SO_4^{2-}-TiO_2 catalysts were 3 times greater than that of P25-TiO_2. Furthermore, the FTIR results showed that there were different groups on the surfaces of the NH_4^+-TiO_2 and SO_4^{2-}-TiO_2 catalysts. To further study the compositions of these catalysts, both NH_4^+-TiO_2 and SO_4^{2-}-TiO_2 were examined by FTIR spectroscopy, giving the spectra shown in Figure 3. In the spectrum of NH_4^+-TiO_2, the broad band between 3000 and 3400 cm^{-1} can be assigned to the stretching vibrations of hydroxyl in Ti−OH and hydroxyl in water, and the band in the range of 1600−1630 cm^{-1} can be attributed to the physically adsorbed surface water.[26] Furthermore, the band occurring between 500 and 800 cm^{-1} can be ascribed to anatase TiO_2.[27,28] Two additional bands in the range of 1200−1800 cm^{-1}, at 1625 and 1400 cm^{-1}, are due to symmetric and asymmetric deformations, respectively, of ammonium ions.[29−31] Therefore, the surface of the NH_4^+-TiO_2 catalyst has basic characteristics. In the spectrum of SO_4^{2-}-TiO_2, bands are present at 904, 981, 1057, 1128, and 1396 cm^{-1}. Both the bands in the low-wavenumber range (900−1300 cm^{-1}) and those in the high-wavenumber range (1300−1400 cm^{-1}) are characteristics of SO_4^{2-}/M_nO_m solid superacids.[42] Therefore, SO_4^{2-}-TiO_2 is an acidic catalyst.

Table 2. Kinetic Data for Photocatalytic Oxidation of CH_3SH (C_0 = 94 ppm) with Different Catalysts Using Three 8-W Black-Light Lamps

			pseudo-first-order kinetics	
catalyst loading (3.93 mg cm^{-2})	relative crystallinity[a]	surface area (m^2 g^{-1})	k_{obs1} (10^{-3} min^{-1})	R
NH_4^+-TiO_2	0.3	169.13	25.47	0.9965
P25-TiO_2	1	50	20.17	0.9998
SO_4^{2-}-TiO_2	0.39	163.14	8.16	0.9990

[a] $I_{A101}/I_{P25-A101}$ = ratio of the anatase 101 peak intensity of the catalyst to that of P25-TiO_2.

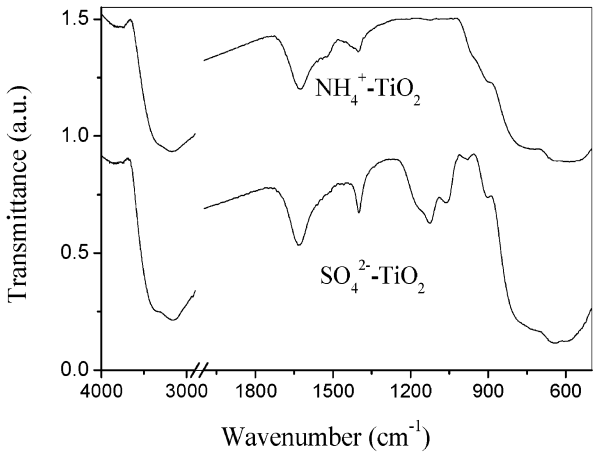

Figure 3. FTIR spectra of NH_4^+-TiO_2 and SO_4^{2-}-TiO_2.

Photocatalytic Oxidation of CH_3SH with Different Photocatalysts. Photocatalytic oxidation under UV-A irradiation initiated by semiconductors is an alternative method to UV-C photolysis for the removal of pollutants from the gas phase. In this study, three black-light lamps were used as a UV-A source to conduct the photocatalytic oxidation of CH_3SH in the synthetic foul gas together with different photocatalysts. Three experiments using NH_4^+-TiO_2, SO_4^{2-}-TiO_2, and P25-TiO_2 catalysts were performed with an initial CH_3SH concentration of 94 ppm and a relative humidity of 60% at room temperature.

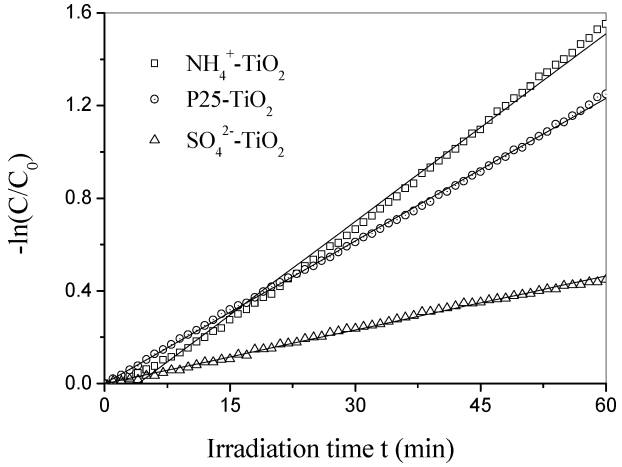

Figure 4. Photocatalytic oxidation of CH_3SH (94 ppm) with different photocatalysts.

Each experiment lasted for 60 min, and the experimental results are presented in Figure 4 and also summarized in Table 2. In this study, the experimental results show that the P25-TiO_2 catalyst can effectively achieve the photocatalytic degradation of CH_3SH in foul gas. Furthermore, the experimental results also indicate that the NH_4^+-TiO_2 catalyst performed better than P25-TiO_2, whereas the SO_4^{2-}-TiO_2 catalyst performed worse. This NH_4^+-modified TiO_2 catalyst had a higher specific surface area than both of the other catalysts, which is beneficial to adsorption. The higher photocatalytic activity of NH_4^+-TiO_2 might result from its surface modification from NH_3 to NH_4^+. According to previous work by us[15] and also by Bashkova et al.,[32] nitrogen groups such as NH_4^+ on the catalyst, with their basic properties, would favor the oxidation of acidic organics such as CH_3SH. On the other hand, SO_4^{2-}-TiO_2 is an acidic catalyst. Although SO_4^{2-}-TiO_2 has an oxidative capability, its surface superacidic properties might not increase the adsorption of CH_3SH, and its low crystallinity is also unfavorable for the photocatalytic oxidation of CH_3SH at room temperature, resulting in a relatively lower photocatalytic activity under these experimental conditions.

The degradation of CH_3SH initiated by reaction with hydroxyl radical has been studied intensively in the past 20 years.[33−37] Recent research has found that the OH• + CH_3SH reaction takes place by forming a weakly bonded complex ($CH_3SH\cdots OH$) first, which presents two hydrogen bonds between the hydroxyl radical and methyl mercaptan. From this complex, two reaction paths diverge: one leading to the abstraction of the hydrogen atom attached to the sulfur atom and the other resulting in hydrogen abstraction of the methyl group. The first channel proceeds much more quickly than the second, and CH_3S• is obtained almost exclusively.[37]

A photocatalytic oxidation process can be initiated by the generation of electron−hole pairs on TiO_2 upon absorption of UV irradiation below 387 nm. When electrons (e^-) and holes (h^+) are photogenerated in the bulk of TiO_2 and move to its surface, the electrons can reduce electron acceptors such as molecular oxygen (O_2), and the holes can oxidize electron donors (such as adsorbed water or hydroxide anion OH^-) to produce active hydroxyl radical (OH•).[38] In this study, the illumination of black-light lamps lies in the range of 310−400 nm with a maximum value at 365 nm, so it can excite TiO_2 to produce these very active electron−hole pairs and achieve the photocatalytic oxidation of CH_3SH. The mechanism of the relevant reactions can be proposed as follows:

$$TiO_2 + h\upsilon \rightarrow TiO_2^* (h_{vb}^+ + e_{cb}^-) \quad (5)$$

$$H_2O_{ads} \leftrightarrow OH^-_{ads} + H^+_{ads} \quad (6)$$

$$h_{vb}^+ + OH^-_{ads} \rightarrow OH\bullet_{ads} \quad (7)$$

$$e_{cb}^- + O_{2\,ads} \rightarrow O_2^-{}_{ads} \quad (8)$$

$$H^+_{ads} + O_2^-{}_{ads} \rightarrow HO_{2\bullet ads} \quad (9)$$

$$CH_3SH_{gas} \leftrightarrow CH_3SH_{ads} \quad (10)$$

$$CH_3SH_{ads} + OH\bullet_{ads} \rightarrow CH_3SH_{ads}\cdots OH_{ads} \rightarrow CH_3S\bullet_{ads} + H_2O_{ads} \quad (11)$$

$$HO_2\bullet + nCH_3SH_{ads} \rightarrow nCH_3S\bullet_{ads} + SO_2 \quad (12)$$

Reaction 11 has been well studied theoretically and also experimentally owing to its importance in atmospheric chemistry. Research has shown that reaction 11 requires little or no activation energy and is very fast and easy.[37] Butkovskaya et al. suggested that the rate constant of reaction 12 should be high because it is an exothermic reaction.[36] Moreover, $CH_3S\bullet_{ads}$ can undergo an oxidation process similar to the photolysis of CH_3SH under UV-C irradiation. Therefore, SO_2 and H_2O are the main final products of the photocatalytic oxidation of CH_3SH over TiO_2. There might be some other intermediates (such as CH_3SSCH_3) during the photocatalytic reaction, but they are all degraded into the products of SO_2, CH_4, and H_2O at the end of the photocatalytic reaction. The mechanisms of production and photocatalytic oxidation of intermediates can be proposed as follows:

$$CH_3S\bullet_{ads} + CH_3S\bullet_{ads} \leftrightarrow CH_3SSCH_{3ads} \quad (13)$$

$$CH_3SSCH_{3ads} + OH\bullet_{ads} \rightarrow CH_3SH_{ads} + CH_3SO\bullet_{ads} \quad (14)$$

$$CH_3SO\bullet_{ads} + OH\bullet_{ads} \rightarrow CH_3SO_2H_{ads} \rightarrow CH_{4ads} + SO_{2ads} \quad (15)$$

Reaction 13 is also exothermic with a reaction heat of −65.4 kcal mol^{-1}, fundamentally as a result of the combination of two radicals.[33] This formation of a disulfide bond is governed by an oxidation/reduction equilibrium[38] and is very important in atmospheric chemistry.[39] Like reaction 13, reaction 15 is also very fast, and its heat of reaction is negative ($\Delta_r H_{298} = -79.7$ kcal mol^{-1}). Thus, the end products of the photocatalytic oxidation of CH_3SH might be SO_2, CH_4, and H_2O, and CH_3SH can be largely degraded.

In general, the oxidation of thiols with molecular oxygen at low temperature is an extremely slow reaction. However, in the presence of basic catalysts, thiol oxidation by air proceeds rapidly.[40−43] Recently, Bashkova et al. reported that surface chemistry, especially surface pH, can influence the adsorption and oxidation of CH_3SH.[44,45] The introduction of nitrogen species onto activated carbons improved the adsorption of CH_3SH significantly, and basic nitrogen groups can act as agents for electron transfer from sulfur to oxygen, which favors the oxidation of CH_3SH.[32] It is known that CH_3SH is sufficiently acidic ($pK_a = 10.3$) to form salts (eq 16) even with weak bases. The thiolate anion (CH_3S^-) is a good electron donor and can react with photogenerated holes (eq 17) or hydroxyl radicals

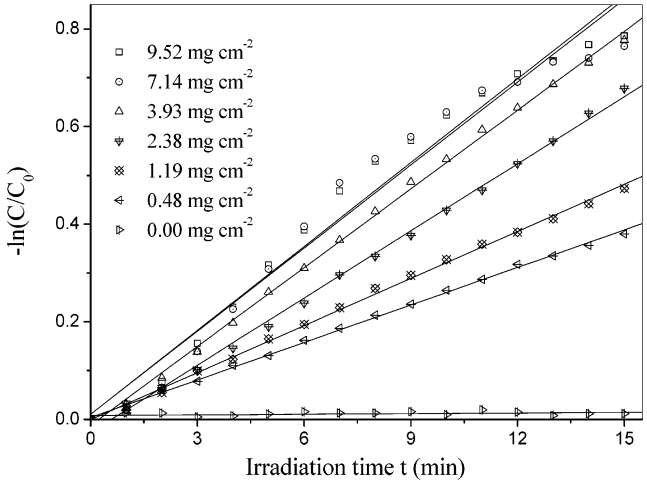

Figure 5. Photocatalytic oxidation of 25 ppm CH_3SH with different amounts of P25-TiO_2.

Table 3. Photocatalytic Oxidation Rate Constants and the Approximate Thicknesses of Catalyst Layers at Different Loadings

catalyst loading (mg cm^{-2})	layer thickness (μm)	removal (%)	k_{obs1} (10^{-3} min^{-1})	R
9.52	1.24	58.24	25.62	0.9991
7.14	3.10	86.26	32.15	0.9990
3.93	6.20	89.21	45.85	0.9986
2.38	10.23	92.26	53.82	0.9992
1.19	18.60	78.73	57.25	0.9878
0.48	24.80	77.88	56.70	0.9810

HO• (eq 18) via electron transfer to give the thiol radical (CH_3S•), which can be photocatalyzed to SO_2, CH_4, and H_2O.

$$CH_3SH_{ads} + OH^-_{ads} \leftrightarrow CH_3S^-_{ads} + H_2O_{ads} \quad (16)$$

$$h_{vb}^+ + CH_3S^-_{ads} \rightarrow CH_3S\bullet_{ads} \quad (17)$$

$$CH_3S^-_{ads} + OH\bullet_{ads} \rightarrow CH_3S\bullet_{ads} + OH^- \quad (18)$$

Because the rates of adsorption and photocatalytic reaction are two critical factors for the degradation of CH_3SH on the catalyst surface, the NH_4^+-modified TiO_2 catalyst demonstrated the most effective removal of CH_3SH by a synergistic effect of adsorption and photocatalytic reaction. Actually, surface modification, compared to inside doping and implanting techniques, is a relatively new approach to enhancing the activity and efficiency of TiO_2 catalysts such as P25-TiO_2. The experimental results in this study indicate that a TiO_2 catalyst with basic functions on its surface such as NH_4^+-TiO_2 might have more commercial interest than pure TiO_2 for the effective adsorption and photocatalytic oxidation of acidic pollutants such as CH_3SH or other thiols.

Effect of Photocatalyst Loading. To further investigate the effects of different experimental factors on the photocatalytic reduction of CH_3SH in foul gas at room temperature, P25-TiO_2 was selected as a standard photocatalyst in the subsequent experiments. The first set of experiments with an initial CH_3SH concentration of 25 ppm was performed under a relative humidity of 60% with different catalyst loadings from 0 to 9.52 mg cm^{-2} on the catalyst fiber sheet (21 cm × 20 cm). The experimental results for this set are shown in Figure 5 and listed in Table 3. The experimental results demonstrated that the rate of CH_3SH reduction increased significantly with increasing photocatalyst loading at the lower level of $<$2.38 mg cm^{-2}.

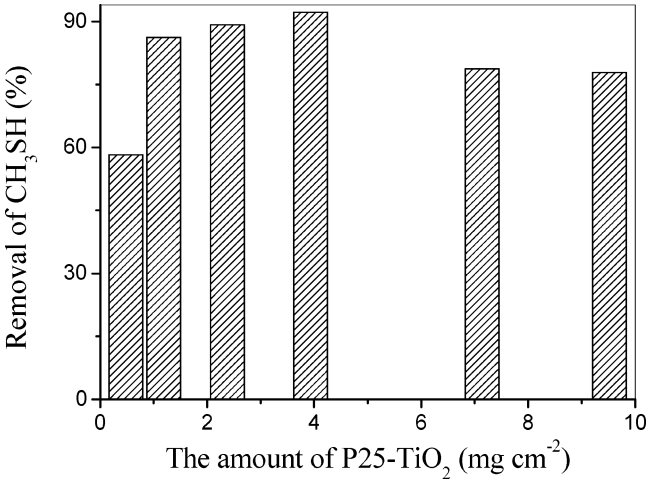

Figure 6. Removal of 25 ppm CH_3SH with different amounts of P25-TiO_2.

However, the further increase of CH_3SH reduction rate became less significant at the higher level from 2.38 to 9.52 mg cm^{-2}. The results showed that the photocatalyst loading of 3.93 mg cm^{-2} achieved the highest CH_3SH removal of 92% after 15 min of photoreaction, as shown in Figure 6. The enhancement of the photocatalytic reaction due to the catalyst loading could be linked to the increase in the effective area of the catalyst under UV irradiation, which would enhance the photon generation rate and thereby yield a faster photocatalytic reaction. However, once the formed catalyst layer reaches a critical thickness, the rates of photon generation and photocatalytic reaction become independent of the catalyst loading.[46] Peral and Ollis reported that 99% of UV light absorption happened within a TiO_2 anatase layer of 4.5 μm;[47] Jacoby et al. suggested that a layer of 2-μm thickness of an opaque catalyst participated in the photoreaction.[48] In this study, it was assumed that the P25-TiO_2 catalyst with an average density of 3.84 g cm^{-3} was uniformly coated on the glass fiber without any interparticle gaps.[49] The thickness of the P25-TiO_2 catalyst layer was determined to be 1.24−24.8 μm for the catalyst loadings of 0.48−9.52 mg cm^{-2}, which might be slightly lower than the actual layer thicknesses. It can be seen that, once the layer thickness is below 4.5 μm, such as 3.1 μm for the catalyst loading of 1.19 mg cm^{-2}, the removal of CH_3SH was lower than 90%. The fact that the catalyst loading of 3.93 mg cm^{-2} with a catalyst layer thickness of about 10 μm achieved the best performance results might indicate that a catalyst layer thickness of around 10 μm is a critical figure under these experimental conditions.

Relative Humidity. To study the effect of relative humidity on CH_3SH removal, a second set of experiments with an initial CH_3SH concentration of 15 ppm and a P25-TiO_2 loading of 3.93 mg cm^{-2} was carried out under various relative humidities in the range of 35−78%. The experimental results for this set are shown in Figure 7 and Table 4. The experiments demonstrated that the highest CH_3SH removal (up to 86%) after 15 min of photocatalytic reaction was achieved under a relative humidity of 43%. Because the removal of CH_3SH in this photoreactor system depends on the rates of both adsorption and photodegradation of CH_3SH on the TiO_2 surface, water is a critical factor affecting both performances.[50−52] CH_3SH (pK_a = 10.3) is able to dissociate when the surface of the adsorbent is highly hydroxylated. In the presence of water vapor, hydroxyl radicals form on the illuminated TiO_2 catalyst to suppress electron−hole recombination because hydroxyl groups or water

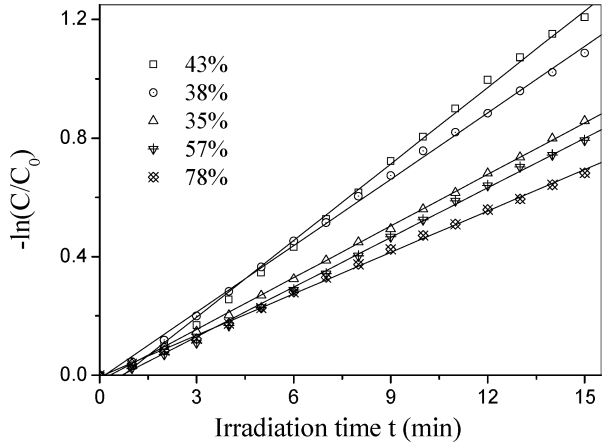

Figure 7. Photocatalytic oxidation kinetics of 15 ppm CH_3SH on supported P25-TiO_2 under different relative humidities.

Table 4. Pseudo-First-Order Kinetic Constant k_{obs} and Relative Coefficient R for the Photocatalytic Oxidation of 15 ppm CH_3SH Using P25-TiO_2 at Different Relative Humidities

RH (%)	k_{obs} (10^{-3} min^{-1})	R
35	58.09	0.9997
38	74.82	0.9992
43	86.16	0.9983
57	55.89	0.9985
78	46.58	0.9994

molecules can behave as hole traps to form surface-adsorbed hydroxyl radicals. The continuous consumption of hydroxyl radicals requires replenishment to maintain photocatalytic activity, only when there is a suitable equilibrium between consumption and adsorption. However, a lower relative humidity might result in a gradual decrease of surface-adsorbed hydroxyl radicals, thus inhibiting the removal of CH_3SH. On the other hand, a higher relative humidity might lead to competitive adsorption between H_2O and CH_3SH on the TiO_2 surface. In addition, excess water might provide recombination centers for electron−hole pairs, which would result in a lower photocatalytic activity in the system. Therefore, the experimental results showed that the removal of CH_3SH increased with increasing relative humidity in the lower range, but decreased with increasing relative humidity in the higher range. It was found that a relative humidity of 43% was an optimal level for the removal of CH_3SH in this synthetic gas phase.

Initial Concentration of CH_3SH. To study the kinetics of the photocatalytic reaction of CH_3SH, a third set of experiments using a catalyst loading of 3.93 mg cm^{-2} under a humidity of 65% at room temperature was performed with different initial concentrations of CH_3SH in the range of 8−95 ppm. The experimental results are shown in Figure 8, in which the experimental data were fitted by applying a pseudo-first-order model to determine an observed rate constant (k_{obs}) of CH_3SH reduction in the experiments as listed in Table 5. It can be seen that the value of the rate constant (k_{obs}) varied significantly with the initial concentration of CH_3SH, from 118 × 10^{-3} min^{-1} at 8 ppm to 20 × 10^{-3} min^{-1} at 95 ppm. The concentration dependence of the k_{obs} value indicates that the photocatalytic degradation of CH_3SH in such a photoreaction system is affected by some competitions. First, the existing water vapor can compete strongly in the adsorption on the TiO_2 surface against CH_3SH. Second, the intermediate products from the initial degradation of CH_3SH can compete

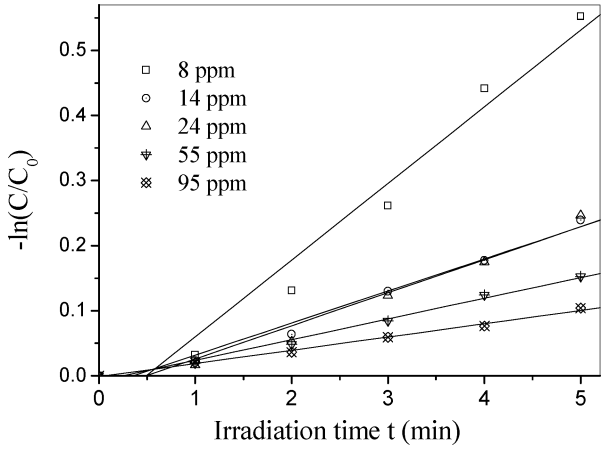

Figure 8. Photocatalytic oxidation of CH_3SH of different initial concentrations.

Table 5. Pseudo-First-Order Kinetic Constant for Photocatalytic Oxidation with Different Initial Concentrations of CH_3SH in the Initial 5 min[a]

initial CH_3SH concentration (ppm)	k_{obs-c} (10^{-3} min^{-1})	R
8	117.79	0.982
14	49.25	0.991
24	50.79	0.982
55	31.75	0.995
95	20.33	0.997

[a] Relative humidity = 65% and P25-TiO_2 amount = 3.93 mg cm^{-2}.

in the consumption of the photogenerated oxidants such as hydroxyl radicals. To better understand the relationship between the adsorption and photocatalytic degradation of CH_3SH in such a photocatalytic reaction system, a detailed kinetic study has been carried out by our research group and will be reported in another article.

Conclusions

This study has confirmed that CH_3SH in a synthetic foul gas can be effectively decomposed by UV-C (<280 nm) photolysis using germicidal lamps, but is resistant to destruction by UV-A (365 nm) photolysis using black-light lamps. The study has also demonstrated that the CH_3SH in foul gas can be successfully degraded by photocatalytic oxidation under UV-A irradiation with a photocatalyst. It was found that the NH_4^+-TiO_2 catalyst achieved a better performance than P25-TiO_2, whereas SO_4^{2-}-TiO_2 demonstrated a poorer performance. The high photocatalytic activity of NH_4^+-TiO_2 for CH_3SH degradation results from its basic properties and a nitrogen group on the NH_4^+-TiO_2 catalyst surface. The experimental results indicate that a catalyst loading of 3.93 mg cm^{-2} and a relative humidity of 43% are two essential factors in achieving the best performance. Under these optimized conditions, the pseudo-first-order kinetic constant k_{obs} for the reduction of CH_3SH with an initial concentration of 15 ppm on P25-TiO_2 was determined to be 86.16 × 10^{-3} min^{-1}. This study was a fundamental research effort to determine the effects of main experimental factors including light wavelength, humidity, catalyst characteristics, and catalyst loading on CH_3SH degradation in a synthetic foul gas. Following the success of this work, it is recommended that odorous gas from a real source such as a refuse collection room or a sewage treatment process can be tested in a continuous-flow pattern to further evaluate the efficiency of this process.

Acknowledgment

This work was financially supported by The Hong Kong Polytechnic University under the ASD project entitled "Development & Optimization of Novel IAQ Technology" (31.37.A508).

Literature Cited

(1) Bashkova, S.; Bagreev, A.; Bandosz, T. J. Adsorption of methyl mercaptan on activated carbons. *Environ. Sci. Technol.* **2002**, *36*, 2777.

(2) Lee, J. H.; Tang, I N. Absolute rate constants for the hydroxyl radical reactions with CH_3SH and C_2H_5SH at room temperature. *J. Chem. Phys.* **1983**, *78*, 6646.

(3) Tsai, Ch. H.; Lee, W. J.; Chen, Ch. Y.; Liao, W. T. Decomposition of CH_3SH in a RF plasma reactor: Reaction products and mechanisms. *Ind. Eng. Chem. Res.* **2001**, *40*, 2384.

(4) Buck, T.; Bohlen, H.; Wöhele, D. Influence of substituents and ligands of various cobalt(II) porphyrin derivatives coordinately bonded to silica on the oxidation of mercaptan. *J. Mol. Catal.* **1993**, *80*, 253.

(5) Chauhan, S. M. S.; Gulati, A.; Sahay, A.; Nizar, P. N. H. Autooxidation of alkyl mercaptans catalysed by cobalt(II) phthalocyanine tetrasodium sulphonate in reverse micelles. *J. Mol. Catal. A: Chem.* **1996**, *105*, 159.

(6) Kastner, J. R.; Das, K. C.; Buquoi, Q.; Melear, N. D. Low temperature catalytic oxidation of hydrogen sulfide and methanethiol using wood and coal fly ash. *Environ. Sci. Technol.* **2003**, *37*, 2568.

(7) Chu, H.; Chu, Y. H.; Chiou, Y. Y.; Horng, K. H.; Tseng, T. K. Catalytic incineration of C_2H_5SH and its mixture with CH_3SH over a Pt/Al_2O_3 catalyst. *J. Environ. Eng.* **2001**, *127*, 438.

(8) Cha, J. M.; Cha, W. S.; Lee, J. H. Removal of organo-sulphur odour compounds by Thiobacillus novellus SRM, sulphur-oxidizing microorganisms. *Process Biochem.* **1999**, *34*, 659.

(9) Mills, B. Review of Methods of Odour Control. *Filtr. Sep.* **1995**, *32*, 147.

(10) Canela, M. C.; Alberici, R. M.; Sofia, R. C. R.; Eberlin, M. N.; Jardim, W. F. Destruction of malodorous compounds using heterogeneous photocatalysis. *Environ. Sci. Technol.* **1999**, *33*, 2788.

(11) Li, F. B.; Li, X. Z.; Hou, M. F. Photocatalytic degradation of 2-mercaptobenzothiazole in aqueous La^{3+}-TiO_2 suspension for odor control. *Appl. Catal. B: Environ.* **2004**, *48*, 185.

(12) Hoffmann, M. R.; Martin, S. T.; Choi, W.; Bahnemannt, D. W. Environmental Applications of Semiconductor Photocatalysis. *Chem. Rev.* **1995**, *95*, 69.

(13) Li, X. Z.; Li, F. B. Study of Au/Au^{3+}-TiO_2 photocatalysts toward visible photooxidation for water and wastewater treatment. *Environ. Sci. Technol.* **2001**, *35*, 2381.

(14) Alberici, R. M.; Jardim, W. F. Photocatalytic destruction of VOC's in the gas-phase using titanium dioxide. *Appl. Catal. B: Environ.* **1997**, *14*, 55.

(15) Li, F. B.; Li, X. Z.; Ao, C. H.; Hou, M. F.; Lee, S. C. Photocatalytic conversion of NO using TiO_2-NH_3 catalysts in ambient air environment. *Appl. Catal. B: Environ.* **2004**, *54*, 275.

(16) Yeung, K. L.; Maira, A. J.; Stolz, J.; Hung, E.; Ho, N. K. Ch.; Wei, A. C.; Soria, J.; Chao, K. J.; Yue, P. L. Ensemble Effects in Nanostructured TiO_2 Used in the Gas-Phase Photooxidation of Trichloroethylene. *J. Phys. Chem. B.* **2002**, *106*, 4608.

(17) Martra, G.; Coluccia, S.; Marchese, L.; Augugliaro, V.; Loddo, V.; Palmisano, L.; Schiavello, M. The role of H_2O in the photocatalytic oxidation of toluene in vapour phase on anatase TiO_2 catalyst: A FTIR study. *Catal. Today.* **1999**, *53*, 695.

(18) Zhao, J.; Yang, X. D. Photocatalytic oxidation for indoor air purification: A literature review. *Build. Environ.* **2003**, *38*, 645.

(19) Segall, J.; Wen, Y.; Singer, R.; Dulligan, M.; Wittig, C. Vibrationally resolved translational energy release spectra from the ultraviolet photodissociation of methyl mercaptan. *J. Chem. Phys.* **1993**, *99*, 6600.

(20) Stevens, J. E.; Jang, H. W.; Butler, L. J.; Light, J. C. An adiabatic model for the photodissociation of CH_3SH in the first ultraviolet adsorption band. *J. Chem. Phys.* **1995**, *102*, 7059.

(21) Balla, R. J.; Heicklen, J. Oxidation of sulfur compounds IV: The photo-oxidation of CH_3SH. *J. Photochem. Photobiol. A* **1985**, *29*, 311.

(22) Mouflih, B.; Larrieu, Ch.; Chaillet, Max. Theoretical study of the photochemical fragmentation of methanethiol. *Chem. Phys.* **1988**, *119*, 221.

(23) Nicovich, J. M.; Kreutter, K. D.; Van Dijk, C. A.; Wine, P. H. Temperature-dependent kinetics studies of the reactions Br ($^2P_{3/2}$) + H_2S ↔ HS + HBr and Br($^2P_{3/2}$) + CH_3SH ↔ CH_3S + HBr. Heats of formation of HS and CH_3S radicals. *J. Phys. Chem.* **1992**, *96*, 2518.

(24) Balla, R. J.; Heicklen, J. Oxidation of sulfur compounds IV: The photo-oxidation of CH_3SH. *J. Photochem.* **1985**, *29*, 311.

(25) Butkovskaya, N. I.; Setser, D. W. Mechanism for the reaction of hydroxyl radicals with dimethyl disulfide. *Chemical Physics Lett.* **1999**, *312*, 37.

(26) Musić, S.; Gotić, M.; Ivanda, M.; Popović, S.; Turković, A.; Trojko, R.; Sekulić, A.; Furić, K. Chemical and microstructural properties of TiO_2 synthesized by sol−gel procedure. *Mater. Sci. Eng. B.* **1997**, *47*, 33.

(27) Phonthammachai, N.; Chairassameewong, T.; Gulari, E.; Jamieson, A. M.; Wongkasemjit, S. Structural and rheological aspect of mesoporous nanocrystalline TiO_2 synthesized via sol−gel process. *Microporous Mesoporous Mater.* **2003**, *66*, 261.

(28) Dvoranová, D.; Brezová, V.; Mazúr, M.; Malati, M. A. Investigations of metal-doped titanium dioxides photocatalysts. *Appl. Catal. B: Environ.* **2002**, *37*, 91.

(29) Ramis, G.; Yi, L.; Busca, G.; Turco, M.; Kotur, E.; Willey, R. J. Adsorption, activation, and oxidation of ammonia over SCR catalysts. *J. Catal.* **1995**, *157*, 523.

(30) Ramis, G.; Larrubia, M. A. An FT-IR study of the adsorption and oxidation of N-containing compounds over Fe_2O_3/Al_2O_3 SCR catalysts. *J. Mol. Catal. A: Chem.* **2004**, *215*, 161.

(31) Konstantin, H. FTIR study of CO and NH_3 co-adsorption on TiO_2 (rutile). *Appl. Surf. Sci.* **1998**, *135*, 331.

(32) Bashkova, S.; Bagreev, A.; Bandosz, T. J. Adsorption/oxidation of CH_3SH on activated carbons containing nitrogen. *Langmuir* **2003**, *19*, 6115.

(33) Hynes, A. J.; Wine, P. H. Kinetics of the hydroxyl radical + methyl mercaptan reaction under atmospheric conditions. *J. Phys. Chem.* **1987**, *91*, 3672.

(34) Tyndall, G. S.; Ravishankara, A. R. Kinetics of the reaction of the methylthio radical with ozone at 298 K. *J. Phys. Chem.* **1989**, *93*, 4707.

(35) Butkovskaya, N. I.; Setser, D. W. Chemical Dynamics of the OH and OD Radical Reactions with H_2S, CH_3SCH_3, and CH_3SH Studied by Infrared Chemiluminescence. *J. Phys. Chem. A.* **1998**, *102*, 6395.

(36) Butkovskaya, N. I.; Setser, D. W. Product Branching Fractions and Kinetic Isotope Effects for the Reactions of OH and OD Radicals with CH_3SH and CH_3SD. *J. Phys. Chem. A.* **1999**, *103*, 6921.

(37) Masgrau, L.; González-Lafont, À.; Lluch, J. M. Variational transition-state theory rate constant calculations of the OH + CH_3SH reaction and several isotope variants. *J. Phys. Chem. A.* **2003**, *107*, 4490.

(38) Li, F. B.; Li, X. J.; Li, X. Z.; Hou, M. F. Photoelectrocatalytic properties and reactivity of Ti/Au−TiO_2 mesh electrodes. *Trans. Nonferrous Met. Soc. China.* **2002**, *12*, 1180.

(39) Benassi, R. Ab initio study of the oxidation of CH_3SH to CH_3SSCH_3. *Theor. Chem. Acc.* **2004**, *112*, 95.

(40) Capaldo, K.; Corbett, J. J.; Kasibhatla, P.; Fischbeck, P.; Pandis, S. N. Effects of ship emissions on sulphur cycling and radiative climate forcing over the ocean. *Nature* **1999**, *400*, 743.

(41) Lucarelli, L.; Nadtochenko, V.; Kiwi, J. Environmental Photochemistry: Quantitative Adsorption and FTIR Studies during the TiO_2−Photocatalyzed Degradation of Orange II. *Langmuir* **2000**, *16*, 1102.

(42) Turk, A.; Sakalls, E.; Lessuck, J.; Karamltsos, H.; Rago, O. Ammonia injection enhances capacity of activated carbon for hydrogen sulfide and methyl mercaptan. *Environ. Sci. Technol.* **1989**, *23*, 1242.

(43) Hou, M. F. Preparation and characterization of porous nanometer-TiO_2 and their photocatalytic oxidation of NOx. *South China Botanical Garden, Chin. Acad. Sci.* **2004**, 48.

(44) Bashkova, S.; Bagreev, A.; Bandosz, T. J. Effect of surface characteristics on adsorption of methyl mercaptan on activated carbons. *Ind. Eng. Chem. Res.* **2002**, *41*, 4346.

(45) Bashkova, S.; Bagreev, A.; Bandosz, T. J. Adsorption of methyl mercaptan on activated carbons. *Environ. Sci. Technol.* **2002**, *36*, 2777.

(46) Ibrahim, H.; de Lasa, H. Photocatalytic conversion of air borne pollutants, effect of catalyst type and catalyst loading in a novel photo-CREC-air unit. *Appl. Catal. B: Environ.* **2002**, *38*, 201.

(47) Peral, J.; Ollis, D. F. Heterogeneous photocatalytic oxidation of gas-phase organics for air purification: Acetone, 1-butanol, butyraldehyde, formaldehyde, and *m*-xylene oxidation. *J. Catal.* **1992**, *136*, 554.

(48) Jacoby, W. A.; Blake, D. M.; Noble, R. D.; Koval, C. A. Kinetics of the Oxidation of Trichloroethylene in Air via Heterogeneous Photocatalysis. *J. Catal.* **1995**, *157*, 87.

(49) Sauer, M. L.; Ollis, D. F. Photocatalytic oxidation of ethanol and acetaldehyde in humidified air. *J. Catal.* **1996**, *158*, 570.

(50) Sang, B. K.; Sung, Ch. H. Kinetic study for photocatalytic degradation of volatile organic compounds in air using thin film TiO_2 photocatalyst. *Appl. Catal. B: Environ.* **2002**, *35*, 305.

(51) Bagreev, A.; Bashkova, S.; Bandosz, T. J. Dual Role of Water in the Process of Methyl Mercaptan Adsorption on Activated Carbons. *Langmuir* **2002**, *18*, 8553.

(52) Coronado, J. M.; Zorn, M. E.; Tejedor-Tejedor, I.; Anderson, M. A. Photocatalytic oxidation of ketones in the gas phase over TiO_2 thin films: A kinetic study on the influence of water vapor. *Appl. Catal. B: Environ.* **2003**, *43*, 329.

Received for review March 15, 2005
Revised manuscript received November 9, 2005
Accepted November 10, 2005

IE050343B